JOURNAL OF DEGRADED AND MINING LANDS MANAGEMENT
Volume 11, Number 3 (April 2024):5585-5596, doi:10.15243/jdmlm.2024.113.5585
ISSN: 2339-076X (p); 2502-2458 (e), www.jdmlm.ub.ac.id

Research Article

Effect of cogongrass biochar enriched with nitrogen fertilizer dissolved in seaweed liquid extract on soil water content of Ultisol

Laode Muhammad Harjoni Kilowasid[1*], Syamsu Alam[2], Tresjia Corina Rakian[1], Nurul Awalia Ansar[1], Nurfadillah[1], Nurfatihah Hijrah Ramdan[1], Irfan Jaya[1], Suryana[1], Widia Agustin[1], Nini Mila Rahni[1], Mashuni[3], La Ode Safuan[1]

[1] Department of Agrotechnology, Halu Oleo University, Jalan HEA Mokodompit 93231, Kendari, South East Sulawesi, Indonesia
[2] Department of Soil Science, Halu Oleo University, Jalan HEA Mokodompit 93231, Kendari, South East Sulawesi, Indonesia
[3] Department of Chemistry, Halu Oleo University, Jalan HEA Mokodompit 93231, Kendari, South East Sulawesi, Indonesia

[*]corresponding author: lohardjoni2@yahoo.co.id

Article history:
Received 25 November 2023
Revised 5 January 2024
Accepted 19 January 2024

Keywords:
biochar
cogongrass
functional group
seaweed extract
soil water retention

Abstract

Ultisol dry land is characterized by significantly low organic carbon content, an important factor influencing soil water content and physico-chemical dynamics. The addition of N fertilizer dissolved in seaweed liquid extract as an enrichment solution can change the character of biochar. Therefore, this study aimed to analyze the characteristics of cogongrass biochar enriched with dissolved N fertilizer in seaweed extract of different species and assess its impact on soil water content in Ultisol. Urea was used as a nitrogen source, and biochar enriched with N fertilizer dissolved in seaweed liquid extract from *Kappapychus alvarezii*, *Sargassum* sp., and *Ulva lactuca* was tested. Biochar dose used was 20% of soil weight with a 10% extract concentration for each type. Furthermore, five-level treatments were tested in a pot experiment, namely (i) without biochar, (ii) biochar unenriched, (iii) enriched with N fertilizer dissolved in *K. alvarezii* extract, (iv) enriched with N fertilizer dissolved in *Sargassum* sp. extract, and (v) biochar enriched with N fertilizer dissolved in *U. lactuca* extract. Each treatment was repeated three times, following a randomized block design. The results showed that cogongrass biochar enriched with N fertilizer dissolved in seaweed extract had a more amorphous surface morphology structure. The proportion of elements and functional groups in cogongrass biochar changed. Enriched biochar increased Ultisol moisture levels, but water holding capacity and retention were lower than the unenriched sample.

To cite this article: Kilowasid, L.M.H., Alam, S., Rakian, T.C., Ansar, N.A., Nurfadillah, Ramdan, N.H., Jaya, I., Suryana, Agustin, W., Rahni, N.M., Mashuni, and Safuan, L.O. 2024. Effect of cogongrass biochar enriched with nitrogen fertilizer dissolved in seaweed liquid extract on soil water content of Ultisol. Journal of Degraded and Mining Lands Management 11(3):5585-5596, doi:10.15243/jdmlm.2024.113.5585.

Introduction

Ultisol is a type of soil covering an area of approximately 45.8 million ha and constitutes the largest part of dry land in Indonesia (Purwanto et al., 2021). The characteristics include high acidity and elevated levels of Al exchange, as well as low nutrient availability and organic carbon content (Buchari et al., 2021). Conventional agricultural activities accelerate soil organic carbon loss from Ultisol in dry land (Giagnoni et al., 2020), significantly impacting content and water holding capacity (Panagea et al., 2021; Sukarman et al., 2022). The quantity of water stored in soil greatly determines the availability for plant

CC BY-NC 4.0 | Attribution-NonCommercial 4.0 International

growth, abundance and activity of soil biota, transformation, and nutrient transport, as well as overall sustainable productivity (Qi et al., 2020; Bai and Cotrufo, 2022; Bian et al., 2022). Based on the derivative impacts caused by the loss of organic carbon, it is necessary to add organic material to sustain soil ecosystem functions, including erosion protection, biodiversity, aggregation, water retention, nutrient cycling, and promotion of plant growth and health (Hoffland et al., 2020). Furthermore, an increase in soil organic carbon can stimulate the hierarchical formation of soil aggregates into various sizes (Yudina and Kuzyakov, 2023). The formation of meso- and macro-aggregates is accompanied by an increase in total porosity through a reduction in the proportion of small pore sizes in soil with a high fine particle fraction content (Jensen et al., 2020; Yang et al., 2021). This increased porosity creates pore spaces in soil that can be occupied by water (Weber et al., 2023). Organic carbon stored between and within soil aggregates contributes significantly to increasing water retention capacity at various levels of water potential (Yang et al., 2014). The hydroxyl (-OH) and carboxyl (-COOH) groups of organic matter play an important role in increasing the capacity to adsorb and retain water (Ding et al., 2006; Zhang et al., 2019).

Presently, porous organic materials rich in hydroxyl and carboxyl groups are frequently used to improve the water-holding performance of degraded soil (Li and Tan, 2021). Biochar, a porous carbon solid substance with a high degree of aromaticity, has hydroxyl and carboxyl groups on its surface as well as strong anti-decomposition ability (Wang et al., 2017). It can be produced from plant biomass through a thermochemical conversion mechanism using pyrolysis methods (Amalina et al., 2022a). The properties include a high organic carbon content, wider specific surface area, cation exchange capacity, nutrient retention capacity, water storage and retention capacity, and a stable structure, which plays an important role in its use as an ameliorant and soil conditioner (Sakhiya et al., 2020). The composition of lignocellulosic materials, including cellulose, hemicellulose, and lignin in the plant biomass greatly determines the character of biochar (Amalina et al., 2022b; Amalina et al., 2022c). Biochar from biomass richer in lignin tends to have a higher surface area and mesopore volume, as well as hydroxyl and carboxyl groups, compared to those rich in cellulose (Gan et al., 2021; Chen et al., 2022; Fan et al., 2022).

Cogongrass vegetation is dominant and widespread on Ultisol dry lands in Indonesia (Susanto and Dwiati, 2022). Biomass of cogongrass mostly contains lignin (Syahrinudin et al., 2020; Madung et al., 2022). Lignin-rich biomass pyrolyzed at 200-400^{o}C will create a pore structure and specific surface area in the resulting biochar, which plays an important role in improving soil water retention (Ma et al., 2019). A previous study (Michael, 2020) found that cogongrass biochar increased pH, organic carbon content, and water holding capacity but not total N in sandy soil. Currently, the role of biochar is evolving toward its use as a biochar-based fertilizer enriched with N solution and liquid organic fertilizer (Karim et al., 2022). Kilowasid et al. (2023) reported that straw rice enriched with the sap of *K. alvarezii* weakened the wave absorption intensity of functional groups associated with -OH stretching on the surface of biochar precursor. It was further explained that the application of enriched biochar increased pH and soil organic carbon content but not the total N in acidic soil. Seaweed *Sargassum* sp., *U. lactuca*, and *K. alvarezii* are dominant in coastal water, specifically in Southeast Sulawesi (Kasim, 2016). Liquid extract contains nutrients and biostimulants which are used as liquid organic fertilizer (Hussain et al., 2021). Therefore, this study aimed to analyze the characteristics of cogongrass biochar enriched with N fertilizer dissolved in the liquid extract of seaweed from the different species and its effect on Ultisol water content.

Materials and Methods

Experiment design

The treatment tested was cogongrass biochar enriched with N fertilizer dissolved in a liquid extract of seaweed from different species, namely *K. alvarezii*, *Sargassum* sp., and *U. lactuca*. Treatment levels consisted of: (i) without biochar (CB0), (ii) biochar without enrichment (CBU0), (iii) biochar enriched with N fertilizer dissolved in extract of *K. alvarezii* (CBUK), (iv) biochar enriched with N fertilizer dissolved in extract of *Sargassum* sp. (CBUS), and (v) biochar enriched with N fertilizer dissolved in extract of *U. lactuca* (CBUU). Biochar dose used was 20% of the soil weight (Michael, 2020), and the extract concentration for each type was 10% (Kilowasid et al., 2023). Each treatment was repeated three times following a randomized block design procedure.

Soil collection

The soil used for this study (an Ultisol) was collected to a depth of 10 cm from the surface. The area of the soil is covered with cogongrass vegetation in Laokke Hamlet, Tanea Village, Konda District, South Konawe Regency, Southeast Sulawesi. The location is at 4^{o}08'06" South Latitude and 122^{o}31'18" East Longitude. The physicochemical properties of soil are presented in Table 1.

Cogongrass biochar production

Cogongrass leaves was collected from cogongrass vegetation distributed in Mokoau village, Kambu District, Kendari City, Southeast Sulawesi Province. The vegetation area is located at S 4^{o}2'19.9284" latitude and E 122^{o}33'3.7944" longitude. The cogongrass leaves were dried in the hot sun for three days, then pyrolyzed at 300-350°C for 1 hour. Biochar was ground and sieved by a 2 mm sieve per opening. Biochar that passed through the

CC BY-NC 4.0 | Attribution-NonCommercial 4.0 International

sieve was stored and further enriched with N fertilizer dissolved in each seaweed liquid extract. Before enrichment, sub-samples of biochar stock were analyzed for pore size using Brunauer Emmet Teller (BET).

Table 1. Physicochemical characteristics of the soil used in the experiment.

Parameters of soil character	Method	Value
Soil particle fraction:		
- Sand (%)	Pippete	8.6
- Silt (%)	Pippete	38.3
- Clay (%)	Pippete	53.1
pH (H_2O)	1:5	4.7
pH (KCl)	1:5	3.7
Organic C (%)	Walkley and Black	1.62
Total N (%)	Kjeldahl	0.15
CN-ratio		10.8
Total P_2O_5 (mg 100 g^{-1})	HCl 25%	22
Total K_2O (mg 100 g^{-1})	HCl 25%	12
Cation exchangeable capacity (cmolc kg^{-1})	NH_4-Acetate 1N, pH7	9.8
Base saturation (%)	NH_4-Acetate 1N, pH7	11
Al^{3+} (cmolc kg^{-1})	KCl 1N	4.28
H^+ (cmolc kg^{-1})	KCl 1N	0.61

Seaweed collection

Fresh seaweed for *U. lactuca* was collected from the landcoast of Tapulaga Village. Additionally, *Sargassum* sp. and *K. alvarezii* were obtained from the coast of Tanjung Tiram and Tondonggeu Village, respectively. Foreign objects attached to each fresh seaweed were removed, cleaned using tap water, and rinsed with distilled water. *U. lactuca* and *Sargassum* sp. were rinsed, spread on the surface of the paper, and dried at room temperature.

Preparation of seaweed extract

The biomass of *U. actuca* and *Sargassum* sp. was dried in the oven for 72 hours at 60°C, ground using a kitchen blender, and sifted through a flour sieve. A total of 100 g of each seaweed powder was placed into a different Erlenmeyer, and reverse osmosis (RO) water was added until the volume reached 1 liter, followed by heating at 60°C, and stirring for 1 hour. The hot slurry obtained was filtered using a filter measuring <0.25 mm opening^{-1} (Hernández-Herrera et al., 2014). Each extract was designated as a stock solution and stored in a different container. Fresh biomass of *K. alvarezii* was washed with tap water to remove surface salts, epiphytes, sand, and dirt, then rinsed with distilled water. The sample was further ground with a kitchen blender without adding water until a slurry mixture was formed. The slurry was filtered using a filter cloth measuring <0.25 mm opening^{-1}, and liquid extract as the stock solution was stored in a plastic container (Pramanick et al., 2020; Vaghela et al., 2023).

Preparation of nitrogen solution in liquid seaweed extract

Liquid extract stock of each seaweed was diluted using RO water to a concentration of 10% (Kilowasid et al., 2023). The source of nitrogen fertilizer was urea (46% N). A total of 20 g was placed into a 1,000 mL Erlenmeyer containing 500 mL of liquid seaweed extract with a concentration of 10% and stirred until all fertilizer particles were dissolved. Subsequently, the liquid extract was added again to reach a volume of 1,000 mL (Liu et al., 2019).

Biochar enrichment with N fertilizer dissolved in seaweed liquid extract

The biochar dose used was 20% of the soil weight (Michael, 2020). Biochar powder that passed through a filter measuring <2 mm hole^{-1} was mixed with N fertilizer treatment dissolved in seaweed liquid extract in a ratio of 1:1 (w v^{-1}).

Analysis of biochar sample

Unenriched and enriched biochar samples were analyzed for surface morphology and element composition using a Scanning Electron Microscope-Energy Dispersive X-ray spectroscopy (SEM-EDS). Functional groups were assessed with a Fourier-Transform Infrared spectrometer (FTIR), and crystal phases were observed using X-ray diffraction (XRD).

Application of biochar enriched into soil

A total of 10 kg Ultisol that passed through a <5 mm sieve was placed into a pot and mixed with the treatment mentioned in the experimental design section. The pots were placed in a greenhouse following a randomized block design. During the incubation period, the soil was not irrigated.

Determination of soil moisture content, soil water holding capacity (SWHC), and retention

After incubation for two weeks, soil samples were taken from each pot to determine water content, water holding capacity, and retention. Soil water content was assessed using the gravimetric method (FAO, 2020). A total of 10 g of fresh soil subsample from each pot was weighed to obtain the wet weight (Ww), then dried at 105°C for 24 hours, and weighed to measure the dry weight (Dw). Soil water content (WC) was determined and expressed in percentages using the formula:

$$\text{WC (\%)} = \frac{\text{Ww} - \text{Dw}}{\text{Dw}} \text{ x } 100$$

A total of 200 g soil subsample from each pot was placed into a PVC tube whose bottom was covered using a 200 mesh nylon sieve and weighed (W_0). Water was added through the top of the tube until it started dripping out through the hole in the nylon cover. When water drips ceased overnight, the weight was measured to obtain the wet weight (Ww). SWHC was estimated using the formula (Lü et al., 2016):

CC BY-NC 4.0 | Attribution-NonCommercial 4.0 International

$$\text{SWHC (\%)} = \frac{\text{Ww} - \text{W}_0}{200} \text{ x } 100$$

Statistical analysis

Data on water content and holding capacity of Ultisol were subjected to a one-way analysis of variance (ANOVA) test. When the treatment showed a significant effect at the level of $p<0.05$, the difference was determined by applying the least significant distance (LSD) at $p<0.05$.

Results

The surface morphology and elemental composition of enriched cogongrass biochar

SEM micrograph (Figure 1) shows that the surface morphology structure of cogongrass biochar (CBU0) has pores arranged similarly to a honeycomb. BET analysis depicted a CBU0 surface area of 111.032 m^2 g^{-1}, pore volume of 4.820 x 10^{-2} cm^3 g^{-1}, and pore radius of 9.234Å. The surface morphology structure of biochar enriched with N fertilizer solution using solvent from extract of *K. alvarezii* (CBUK), *Sargassum* sp. (CBUS), as well as *U. lactuca* (CBUU), showed visible dried droplets covering the surface of the pores. Consequently, the surface shape appeared to be more amorphous.

EDS analysis using the mapping method (Figure 2) showed that the proportion of element C in CBU0 was the most dominant. The abundance decreased with the addition of N fertilizer dissolved in extract from each seaweed, with the greatest reduction occurring in CBUU. The proportion of element O was more dominant in CBUK and CBUU, while that of CBUS was less than in CBU0. The largest increase in the proportion of O occurred in CBUU. Furthermore, the composition of Mg, Al, and Si elements in CBU0 increased with the addition of N fertilizer solution as a solvent for all seaweed extract. The largest increase for Mg and Al occurred in CBUU, while CBUK had the highest Si proportion.

The addition of N fertilizer dissolved in an extract from *K. alvarezii* and *Sargassum* sp. increased the proportion of Cl element in biochar precursor (CBU0), and the largest increase occurred in CBUK. The proportion of P element from CBU0 with the addition of N fertilizer solution using *U. lactuca* extract as solvent increased, compared to the sample prepared with solvents from other extract, which declined slightly. The K and Ca composition in CBU0 increased with the addition of an N fertilizer solution using solvents from the extract of the three seaweed species, with the largest change occurring in CBUK. There was a large proportion of Fe in CBUK, but the element in CBU0 was minimal (not detected).

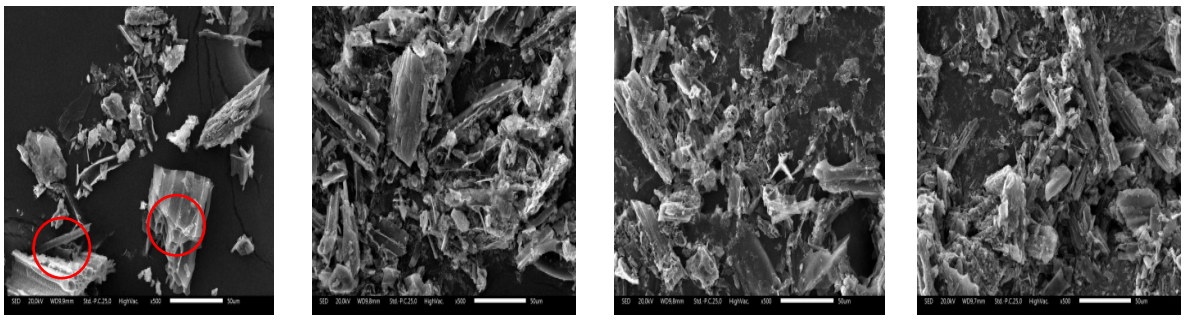

(A) (B) (C) (D)

Figure 1. SEM images of (A) unenriched cogongrass biochar (CBU0), (B) cogongrass biochar enriched with N fertilizer dissolved in *K.. alvarezii* extract (CBUK), (C) cogongrass biochar enriched with N fertilizer dissolved in *Sargassum* sp. extract (CBUS), and (D) cogongrass biochar enriched N fertilizer dissolved in *U. lactuca* extract (CBUU).

The functional groups of enriched biochar

The FTIR spectrum (Figure 3) shows nine wavenumber peaks at CBU0, eight for CBUU, and six for both CBUK and CBUS. Peaks in the wave number range <500, 1,000-1,200, 1,400-15,000, 1,550-1,670, and 3,200-3,700 cm^{-1} were detected for all biochar treatments. The peak wave number of 693.32 cm^{-1} was only detected at CBUU, while those in the range of 750-800 cm^{-1} were found in CBU0 and CBUU. Peaks in the wavenumber region of 850-900 cm^{-1} were detected in CBU0, CBUK, and CBUU, while the peak at 2068.05 cm^{-1} was only recorded in CBUS. Peak wave numbers of 3,849.03 and 3,863.47 cm^{-1} were only found in CBU0.

XRD of enriched biochar

XRD patterns of all biochar (Figure 4) show crystal peaks. The most prominent peak intensity occurred in the diffraction area (2 theta) at 20-30 degrees, followed by 35-50 degrees and 52-70 degrees. The crystal and amorphous fractions in CBU0 were 15.45% and 84.55%, while those of CBUK, CBUS, and CBUU were 16.05% and 83.92%, 11.30% and 88.70%, as well as 14.38% and 85.62%, respectively (Table 2).

CC BY-NC 4.0 | Attribution-NonCommercial 4.0 International

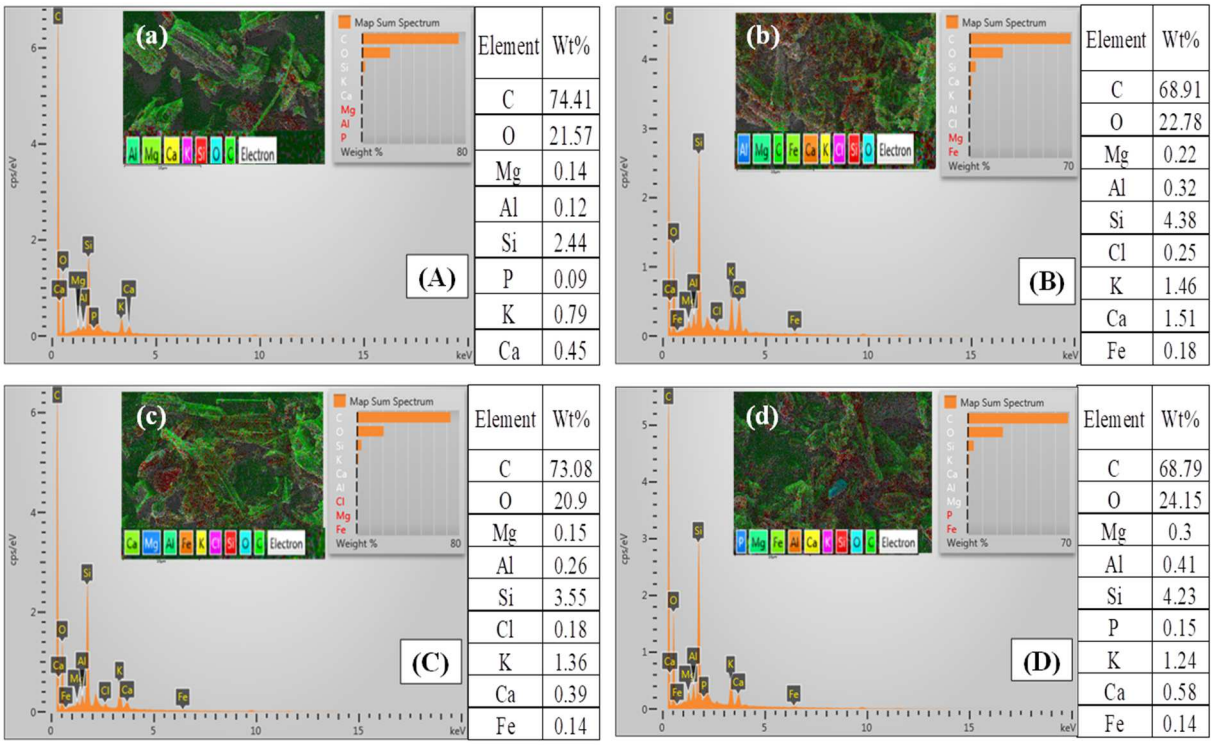

Element	Wt%
C	74.41
O	21.57
Mg	0.14
Al	0.12
Si	2.44
P	0.09
K	0.79
Ca	0.45

Element	Wt%
C	68.91
O	22.78
Mg	0.22
Al	0.32
Si	4.38
Cl	0.25
K	1.46
Ca	1.51
Fe	0.18

Element	Wt%
C	73.08
O	20.9
Mg	0.15
Al	0.26
Si	3.55
Cl	0.18
K	1.36
Ca	0.39
Fe	0.14

Element	Wt%
C	68.79
O	24.15
Mg	0.3
Al	0.41
Si	4.23
P	0.15
K	1.24
Ca	0.58
Fe	0.14

Figure 2. Elemental composition of: (A) unenriched cogongrass biochar (CBU0), (B) enriched with N fertilizer dissolved in the extract of *K. alvarezii* (CBUK), (C) enriched with N fertilizer dissolved in the extract of *Sargassum* sp. (CBUS), and (D) enriched N fertilizer dissolved in the extract of *U. lactuca* solvent (CBUU). Insertions (a), (b), (c), and (d) revealed SEM-EDS elemental mapping analysis of the cogongrass biochar area.

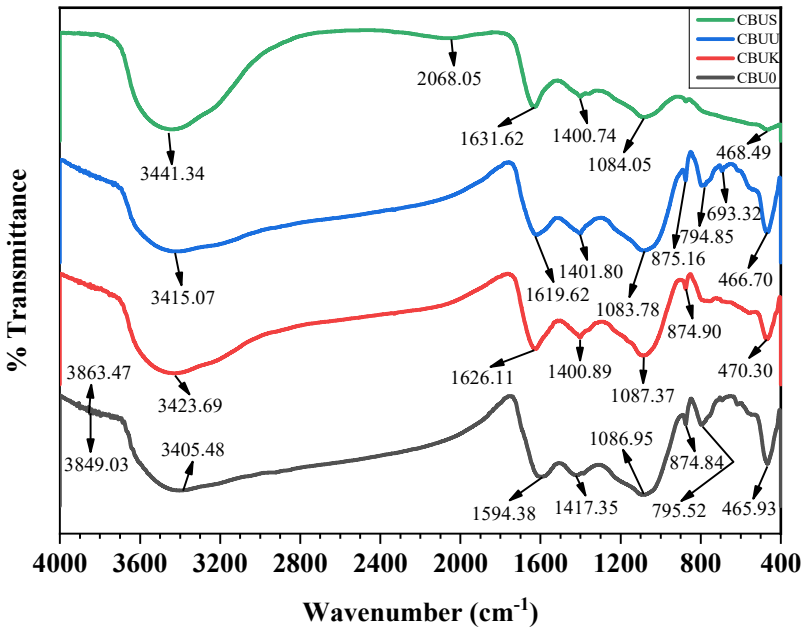

Figure 3. FTIR- spectra of cogongrass biochar enriched with N fertilizer dissolved in seaweed liquid extract of different types.

CC BY-NC 4.0 | Attribution-NonCommercial 4.0 International

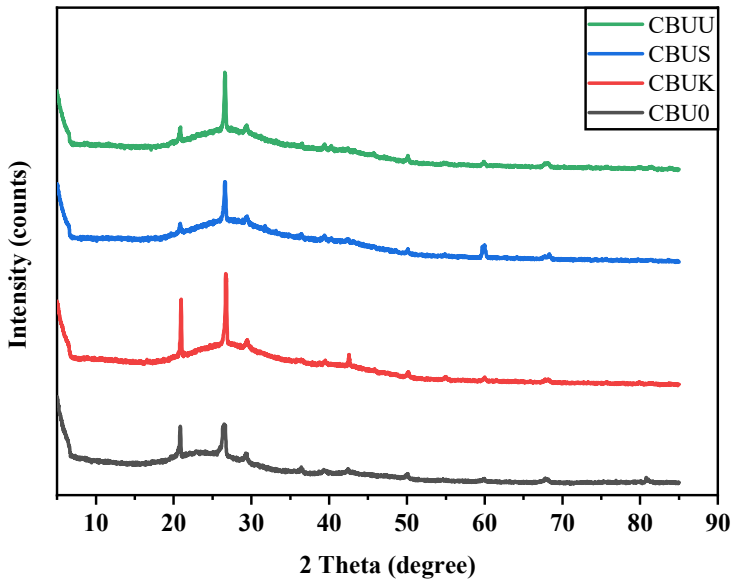

Figure 4. XRD pattern of cogongrass biochar enriched with nitrogen fertilizer dissolved in the liquid extract of different seaweed species.

Table 2. Crystalline and amorphous fractions for cogongrass biochar treatment.

Treatments	Crystalline (%)	Amorphous (%)
CBU0	15.45	84.55
CBUK	16.05	83.92
CBUS	11.30	88.70
CBUU	14.38	85.62

Soil moisture content, water holding, and retention capacity

ANOVA showed that cogongrass biochar treatment enriched with N fertilizer dissolved in seaweed extract had a significant effect ($df_{(4;8)}$, F = 17.166 at the p = 0.001 level) on soil moisture content after two weeks of incubation. Soil moisture content in CBUK was the highest and was significantly different ($p<0.05$) compared to CB0 and CBU0, but not significantly different from CBUS and CBUU ($p<0.05$). The difference between CBUS and CBUU compared to CB0 and CBU0 was significant ($p<0.05$), while that of CB0 and CBU0 was not (Figure 5). ANOVA showed that cogongrass biochar enriched with N fertilizer dissolved in seaweed extract had a significant effect (df(4;8), F = 30.741 at p = 0.000) on SWHC. The highest SWHC was found in CBU0 and significantly different (LSD at $p<0.05$) compared to other treatments. The difference between CB0, CBUK, CBUS, and CBUU was not significant (Figure 6).

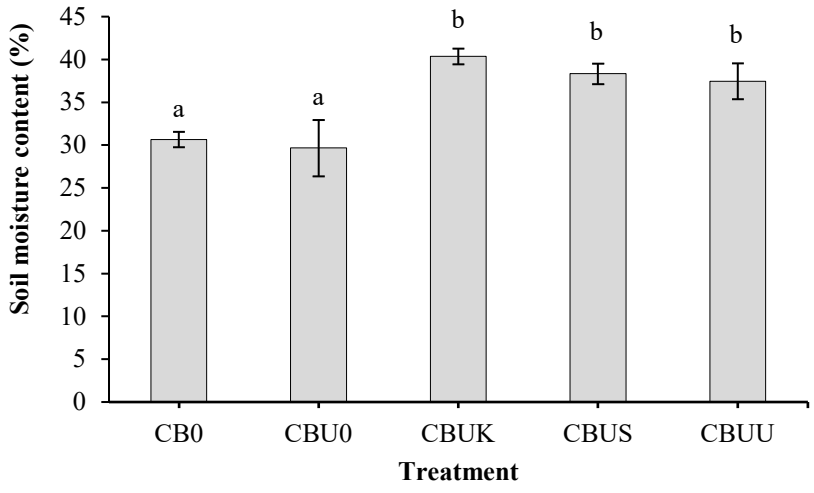

Figure 5. Differences in soil moisture content among cogongrass biochar enriched with N fertilizer dissolved in seaweed extract of different species. Different letters above the error bar show significant differences according to the LSD test at the $p<0.05$ level.

CC BY-NC 4.0 | Attribution-NonCommercial 4.0 International

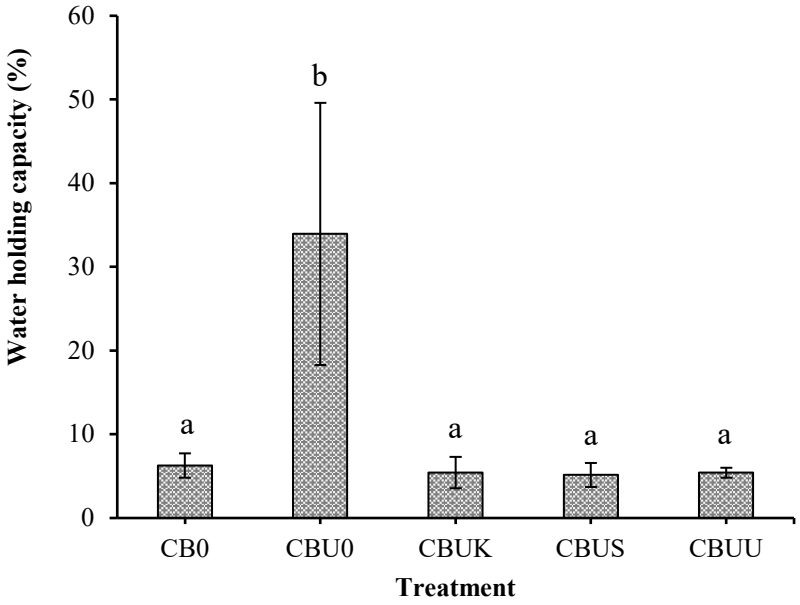

Figure 6. Differences in SWHC among cogongrass biochar enriched with N fertilizer dissolved in seaweed extract of different species. Different letters above the error bar show significant differences according to the LSD test at the $p<0.05$ level.

Figure 7 shows that soil water retention in CBUO was higher than in CB0, CBUK, CBUS, and CBUU. The next day, after the soil was saturated, the amount of water retained in CBUO was 71%, while that of CB0, CBUK, CBUS, and CBUU was 12, 9, 8, and 11%, respectively. Water loss in CB0 was faster than in CBUK, CBUS, and CBUU, while that of CBUO was significantly slower than that of other treatments. Water retained by the CBUO treatment was 30%, while others had reached 0% on the seventh day after the soil was saturated.

The quantity of water retained in CB0 reached 0% on the second day, while that of CBUK, CBUS, and CBUU treatments occurred on the 6-7th day. Water retention in the CBU0 treatment remained at 10% up to the 14th day.

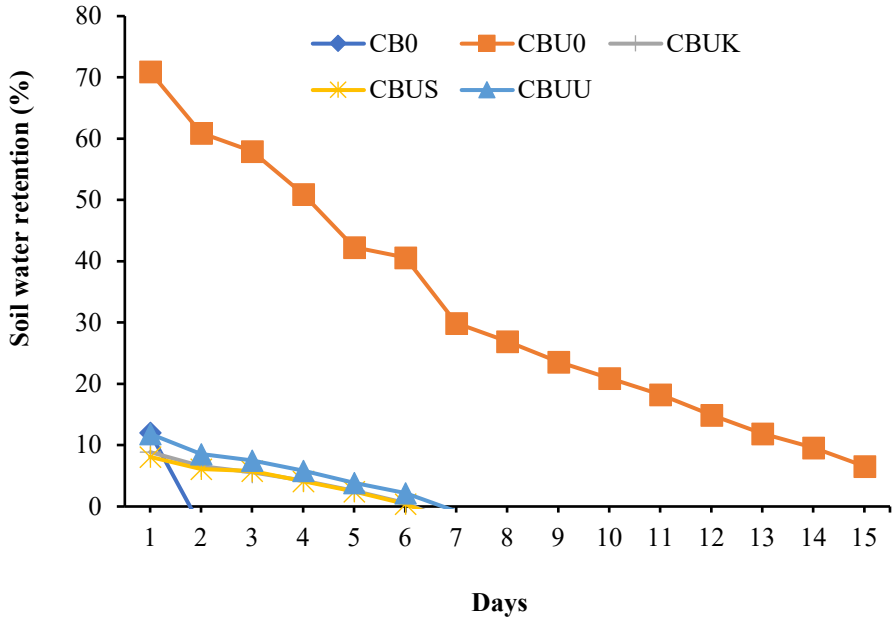

Figure 7. Soil water retention capacity between cogongrass biochar enriched with N fertilizer dissolved in seaweed extract of different species.

CC BY-NC 4.0 | Attribution-NonCommercial 4.0 International

Discussion

Characteristics of enriched biochar

The SEM image (Figure 1) showed that cogongrass biochar had a honeycomb-like arrangement of pores, with a surface area of 111.032 m^2 g^{-1}, a volume of 4.820 x 10^{-2} cm^3 g^{-1}, and a diameter of 0.923 nm. The pores were produced through the C gasification mechanism during combustion, which created the surface area and porous nature of biochar (Singh et al., 2021). These properties play an important role in the adsorption of organic compounds (Huang et al., 2023). According to previous studies, organic compounds from seaweed extract are stored in hydrocolloids (carrageenan) and alginates (hydrogel), which are capable of forming gels (Lee and Mooney, 2012; Martín-del-Campo et al., 2021). These hydrocolloid and hydrogel materials can cover the surface pores of biochar. This was depicted through the SEM image in Figure 1, illustrating that the surface pores of cogongrass biochar precursor became invisible after the addition of N fertilizer solution with liquid extract solvents from the three seaweed species.

Seaweed extract contains phenolic compounds, flavonoids, steroids, saponins, and quinones (Rajivgandhi et al., 2021; Vaghela et al., 2023). The functional groups of these compounds can interact with those on the surface of biochar, eventually changing the degree of crystallization. XRD pattern analysis showed that the amorphous phase fraction for precursor and enriched biochar was > 80%, while the crystal phase was < 20% (Table 2). The peak intensity of XRD (Figure 4) in the diffraction area of 20-300 shows the presence of various silica crystals, 35-500 represents calcite, and 55-820 implies the presence of Fe, magnetite, and aluminum crystals (Dorset, 1998; Ilkiv et al., 2015; Clemente et al., 2018; Nain et al., 2022). The occurrence of various silica crystals was related to the proportion of the element Si as the most dominant compared to other metals in all biochar, both precursor and enriched (Table 1). Other metal elements detected were Al, Mg, Ca, and K, while Fe was only discovered in biochar after the addition of N fertilizer solution using extract solvent from *K. alvarezii*, *Sargassum* sp., and *U. lactuca* (Table 1). The interaction of the Si element with each of these metal elements can form Al-silicate, Mg-silicate, Ca-silicate, K-silicate, and Fe-silicate crystals (Niu et al., 2019; Sornhiran et al., 2022). This caused the crystal phase to follow the character of silica crystals formed with other metal elements, specifically K in cogongrass biomass and biochar (Kow et al., 2014). The dominance of the amorphous nature in all biochar treatments was closely related to the content of lignin, hemicellulose, cellulose, and other organic components (Sackey et al., 2021). This nature plays an important role in water adsorption capacity (Kulasinski et al., 2015), which is determined by the abundance of hydrophobic and hydrophilic functional groups (Drahorad et al., 2020).

FTIR spectrum analysis (Figure 3) showed that the peak below the wave number 500 cm^{-1} was related to the C-X stretching vibration of halocarbon compounds, including organofluorine, organochlorine, organobromine, and organoiodine (Waqas et al., 2018; Mujtaba et al., 2021). As shown in Figure 2, the proportion of Cl elements increased with the addition of N fertilizer solution using solvents from liquid extract of *Sargassum* sp., and *K. alvarezii*. This increase triggered an elevation in the absorption band intensity from the peak wave number of 465.93 cm^{-1} to 468.69 cm^{-1} with the addition of N fertilizer solution prepared using solvent from *Sargassum* sp. extract, while *K. alvarezii* extract caused a rise to 470.30 cm^{-1} (Figure 3). These peaks showed the presence of organochlorine compounds.

The peak wave number of 693.32 cm^{-1} was related to aromatic C-H out-of-plane bending (Nandiyanto et al., 2019), and this was only found in cogongrass biochar added with N fertilizer solution of *U. lactuca* extract as a solvent (Figure 3). This means that the addition of the solution introduced new functional groups. The peak wave number of 795.52 cm^{-1} was detected in cogongrass biochar, and 794.85 cm^{-1} was found in the sample treated with N fertilizer solution using *U. lactuca* extract solvent, showing the presence of bending vibrations from the C-H, Si-H and CH_3 groups (Bashir et al., 2018; Wystalska and Kwarciak-Kozlowska, 2021), These results implied that the addition of N fertilizer solution with extract solvents from *K. alvarezii* and *Sargassum* sp. could change the structure of functional groups associated with C-H, Si-H and CH_3 and cogongrass biochar, while the addition *U. lactuca* extract solvent had no effect.

A wave number with a peak of 874.84 cm^{-1} was detected in cogongrass biochar, 874.90 cm^{-1} in the sample with N fertilizer solution of extract solvent from *K. alvarezii*, as well as 875.16 cm^{-1} in extract solvent from *U. lactuca* (Figure 3). These peaks show the presence of C-N/R-O-C/R-O-CH_3 stretching aromatic C-H (Zhao et al., 2019; Phuong and Loc, 2022). The wave number peaks associated with these groups were eliminated from cogongrass biochar added with N fertilizer solution using *Sargassum* sp. extract solvent. Conversely, a new functional group was detected at the wave number peak of 2068.05 cm^{-1} (Figure 3) related to C≡C stretching vibrations, showing the presence of alkyne functional groups (Hidayat et al., 2021).

Cogongrass biochar, both with and without enrichment, had peaks in the wave number areas 1000-1200, 1400-1500, and 1550-1670 cm^{-1} (Figure 3) related to the presence of the C=O/C-O-C (Zhao et al., 2019), N-H (Nazri et al., 2023), and C=C group respectively (Nandiyanto et al., 2019). This means that the addition of N fertilizer solution with solvent extract did not change the structure of the groups associated with C=O, N-H deformation, and C=C from the surface of biochar.

CC BY-NC 4.0 | Attribution-NonCommercial 4.0 International

Peaks in the wavenumber range of 3,200-3,700 cm^{-1} were detected in all biochar (Figure 3), showing the presence of functional groups associated with O–H stretching of H-bonded hydroxyl groups (Zhao et al., 2019; Janu et al., 2021). Moreover, peak wave numbers 3,849.03 cm^{-1} and 3,863.47 cm^{-1} were only detected in cogongrass biochar. These two wave numbers were associated with the presence of hydroxyl groups (Nandiyanto et al., 2019). This showed that the hydrophobic properties of biochar were lower compared to when N fertilizer solution was added with solvent extract. This reduction may be related to the formation of a film-like layer on the surface of biochar grains by the gel carried by seaweed extract (Shitole et al., 2014; Yaich et al., 2014).

Effect of biochar enrichment on Ultisol characteristics

The results showed that soil moisture levels increased significantly after administering cogongrass biochar enriched with N fertilizer solution of extract solvents from *K. alvarezii*, *Sargassum* sp., and *U. lactuca* compared to without biochar, and enrichment (Figure 5). Soil moisture content increased by 7-10% of cogongrass biochar enriched with N fertilizer solution of extract solvents from *K. alvarezii*, *Sargassum* sp., and *U. lactuca* compared to soil without biochar, and 8-11% of the cogongrass biochar enriched compared to soil with cogongrass biochar. This increase showed that seaweed extract played an important role as a solvent for N fertilizer. Wadduwage et al. (2023) found that the application of seaweed extract increased soil moisture levels. The polysaccharide content in the gel that covered biochar has water-adsorbing properties (Chudasama et al., 2022).

In this study, it was found that water-storing capacity in soil with the addition of cogongrass biochar increased 5.41 times compared to the control, while the addition of N fertilizer solution with liquid extract solvent to cogongrass biochar reduced the ability of the cogongrass biochar to hold water in the soil (Figure 6). The reduction was attributed to the loss of hydroxyl and carboxyl groups as well as the closing of the pores on the biochar surface. FTIR analysis (Figure 3) showed that the presence of N fertilizer solution from seaweed extract solvent eliminated the wave number peak associated with the hydroxyl group. This resulted in a decreased capacity of cogongrass biochar precursor to adsorb water (Cole et al., 2019; Yaashikaa et al., 2020). Biochar porosity also contributed greatly to increasing water-holding capacity (Kinney et al., 2012). This increase could be related to the presence of pore space from biochar (Batista et al., 2018). As stated by Hussain et al., 2020), the addition of biochar increased the water retention capacity of the soil, regardless of the dominant particle fraction, whether sand, silt, or clay. In this study, the addition of biochar increased the water-holding capacity of the soil (Figure 7), with a fine particle fraction (silt+clay) reaching 91.4% (Table 1). Figure 7 also shows that the amount of water retained until the seventh day was 29.92%. For soil enriched with N fertilizer solution from seaweed liquid extract, the quantity of water retained was below 1% on the seventh day, while for soil without cogongrass biochar with or without enrichment, it decreased below 1% on the first day. This means that the enrichment significantly reduced the ability of cogongrass biochar to increase water-holding capacity. This decrease was related to the presence of a film-like layer of dried seaweed extract gel droplets, which acted as a barrier to prevent water from entering the pores.

Conclusion

The use of N fertilizer dissolved in a liquid extract of *Sargassum* sp., *U. lactuca*, and *K. alvarezii* as enrichment solutions changed the chemical element composition, morphological structure, and functional groups on the cogongrass biochar surface. These changes led to a reduction in the hydrophobic properties, impacting the ability to increase the water holding and retention capacity of Ultisol. However, further studies are needed to examine changes in the character of biochar enriched with this solution over time and its impact on the availability of water and nutrients for plants in Ultisol dry land.

Acknowledgments

The authors are grateful to the Directorate of Research, Technology and Community Service, Directorate General of Higher Education, Research and Technology for funding this study through contract number 123/E5/PG.02.00PL/2023. The authors are also grateful to the National Research and Innovation Agency for assisting in analyzing samples using FTIR, XRD, SEM-EDS, and BET.

References

Amalina, F., Razak, A.S.A., Krishnan, S., Sulaiman, H., Zularisam, A.W. and Nasrullah, M. 2022a. Biochar production techniques utilizing biomass waste-derived materials and environmental applications – A review. *Journal of Hazardous Materials Advances* 7:100134, doi:10.1016/j.hazadv.2022.100134.

Amalina, F., Razak, A.S.A., Krishnan, S., Zularisam, A.W. and Nasrullah, M. 2022b. A comprehensive assessment of the method for producing biochar, its characterization, stability, and potential applications in regenerative economic sustainability – A review. *Cleaner Materials* 3:100045, doi:10.1016/j.clema.2022.100045.

Amalina, F., Syukor Abd Razak, A., Krishnan, S., Sulaiman, H., Zularisam, A.W. and Nasrullah, M. 2022c. Advanced techniques in the production of biochar from lignocellulosic biomass and environmental applications. *Cleaner Materials* 6:100137, doi:10.1016/j.clema.2022.100137.

Bai, Y. and Cotrufo, M.F. 2022. Grassland soil carbon sequestration: current understanding, challenges, and solutions. *Science* 377(6606):603-608, doi:10.1126/science.abo2380.

CC BY-NC 4.0 | Attribution-NonCommercial 4.0 International

Bashir, S., Zhu, J., Fu, Q. and Hu, H. 2018. Comparing the adsorption mechanism of Cd by rice straw pristine and KOH-modified biochar. *Environmental Science and Pollution Research* 25:11875-11883, doi:10.1007/s11356-018-1292-z.

Batista, E.M.C.C., Shultz, J., Matos, T.T.S., Fornari, M.R., Ferreira, T.M., Szpoganicz, B., De Freitas, R.A. and Mangrich, A.S. 2018. Effect of surface and porosity of biochar on water holding capacity aiming indirectly at preservation of the Amazon biome. *Scientific Reports* 8:10667, doi:10.1038/s41598-018-28794-z.

Bian, H., Li, C., Zhu, J., Xu, L., Li, M., Zheng, S. and He, N. 2022. Soil moisture affects the rapid response of microbes to labile organic C addition. *Frontiers in Ecology and Evolution* 10:857185, doi:10.3389/fevo.2022.857185.

Buchari, H., Untari, T., Niswati, A. and Sunyoto, S. 2021. Change of soil biomass carbon microorganism in Ultisols soil due to application of humic acid and phosphate fertilization. *Journal of Tropical Soils* 26(3):149-156, doi:10.5400/jts.2021.v26i3.149-156.

Chen, D., Cen, K., Zhuang, X., Gan, Z., Zhou, J., Zhang, Y. and Zhang, H. 2022. Insight into biomass pyrolysis mechanism based on cellulose, hemicellulose, and lignin: evolution of volatiles and kinetics, elucidation of reaction pathways, and characterization of gas, biochar and bio-oil. *Combustion and Flame* 242:112142, doi:10.1016/j.combustflame.2022.112142.

Chudasama, N.A., Polisetti, V., Maity, T.K., Reddy, A.V.R. and Prasad, K. 2022. Preparation of seaweed polysaccharide based hydrophobic composite membranes for the separation of oil/water emulsion and protein. *International Journal of Biological Macromolecules* 199:36-41, doi:10.1016/j.ijbiomac.2021.12.087.

Clemente, J. S., Beauchemin, S., Thibault, Y., Mackinnon, T. and Smith, D. 2018. Differentiating inorganics in biochars produced at commercial scale using principal component analysis. *ACS Omega* 3(6):6931-6944, doi:10.1021/acsomega.8b00523.

Cole, E.J., Zandvakili, O.R., Xing, B., Hashemi, M., Herbert, S. and Mashayekhi, H.H. 2019. Dataset on the effect of hardwood biochar on soil gravimetric moisture content and nitrate dynamics at different soil depths with FTIR analysis of fresh and aged biochar. *Data in Brief* 25:104073, doi:10.1016/j.dib.2019.104073.

Ding, G., Liu, X., Herbert, S., Novak, J., Amarasiriwardena, D. and Xing, B. 2006. Effect of cover crop management on soil organic matter. *Geoderma* 130(3-4):229-239, doi:10.1016/j.geoderma.2005.01.019.

Dorset, D.L. 1998. X-ray diffraction: A practical approach. *Microscopy and Microanalysis* 4(5):513-515, doi:10.1017/S143192769800049X.

Drahorad, S.L., Jehn, F.U., Ellerbrock, R.H., Siemens, J. and Felix-Henningsen, P. 2020. Soil organic matter content and its aliphatic character define the hydrophobicity of biocrusts in different successional stages. *Ecohydrology* 13(6):e2232, doi:10.1002/eco.2232.

Fan, M., Li, C., Shao, Y., Zhang, S., Gholizadeh, M. and Hu, X. 2022. Pyrolysis of cellulose: Correlation of hydrophilicity with evolution of functionality of biochar. *Science of The Total Environment* 825:153959, doi:10.1016/j.scitotenv.2022.153959.

FAO. 2020. Soil testing methods - Global Soil Doctors Programme - A farmer to farmer training programme. Soil testing methods manual.

Gan, F., Cheng, B., Jin, Z., Dai, Z., Wang, B., Yang, L. and Jiang, X. 2021. Hierarchical porous biochar from plant-based biomass through selectively removing lignin carbon from biochar for enhanced removal of toluene. *Chemosphere* 279:130514, doi:10.1016/j.chemosphere.2021.130514.

Giagnoni, L., Taiti, C., León, P., Costa, C., Menesatti, P., Espejo, R., Gómez-Paccard, C., Hontoria, C., Vázquez, E., Benito, M., Mancuso, S. and Renella, G. 2020. Volatile organic compound emission and biochemical properties of degraded Ultisols ameliorated by no tillage and liming. *Pedosphere* 30(5):597-606, doi:10.1016/S1002-0160(20)60024-8.

Hernández-Herrera, R.M., Santacruz-Ruvalcaba, F., Ruiz-López, M.A., Norrie, J. and Hernández-Carmona, G. 2014. Effect of liquid seaweed extracts on growth of tomato seedlings (*Solanum lycopersicum* L.). *Journal of Applied Phycology* 26(1):619-628, doi:10.1007/s10811-013-0078-4.

Hidayat, S., Bakar, M.S.A., Ahmed, A., Iryani, D.A., Hussain, M., Jamil, F. and Park, Y.K. 2021. Comprehensive kinetic study of Imperata Cylindrica pyrolysis via Asym2sig deconvolution and combined kinetics. *Journal of Analytical and Applied Pyrolysis* 156:103133, doi:10.1016/j.jaap.2021.105133.

Hoffland, E., Kuyper, T.W., Comans, R.N.J. and Creamer, R.E. 2020. Eco-functionality of organic matter in soils. *Plant and Soil* 455(1-2):1-22, doi:10.1007/s11104-020-04651-9.

Huang, B., Huang, D., Zheng, Q., Yan, C., Feng, J., Gao, H., Fu, H. and Liao, Y. 2023. Enhanced adsorption capacity of tetracycline on porous graphitic biochar with an ultra-large surface area. *RSC Advances* 13(15):10397-10407, doi:10.1039/d3ra00745f.

Hussain, H.I., Kasinadhuni, N. and Arioli, T. 2021. The effect of seaweed extract on tomato plant growth, productivity and soil. *Journal of Applied Phycology* 33(2):1305-1315, doi:10.1007/s10811-021-02387-2.

Hussain, R., Ravi, K. and Garg, A. 2020. Influence of biochar on the soil water retention characteristics (SWRC): potential application in geotechnical engineering structures. *Soil and Tillage Research* 204:104713, doi:10.1016/j.still.2020.104713.

Ilkiv, B., Petrovska, S., Sergiienko, R., Foya, O., Ilkiv, O., Shibata, E., Nakamura, T. and Zaulychnyy, Y. 2015. Electronic structure of hollow graphitic carbon nanoparticles fabricated from acetylene carbon black. *Fullerenes Nanotubes and Carbon Nanostructures* 23(5):449-454, doi:10.1080/1536383X.2014.885957.

Janu, R., Mrlik, V., Ribitsch, D., Hofman, J., Sedláček, P., Bielská, L. and Soja, G. 2021. Biochar surface functional groups as affected by biomass feedstock, biochar composition and pyrolysis temperature. *Carbon Resources Conversion* 4:36-46, doi:10.1016/j.crcon.2021.01.003.

Jensen, J.L., Schjønning, P., Watts, C.W., Christensen, B. T. and Munkholm, L.J. 2020. Short-term changes in soil pore size distribution: Impact of land use. *Soil and Tillage Research* 199:104597, doi:10.1016/j.still.2020.104597.

Karim, A.A., Kumar, M., Singh, E., Kumar, A., Kumar, S., Ray, A. and Dhal, N.K. 2022. Enrichment of primary macronutrients in biochar for sustainable agriculture: a review. *Critical Reviews in Environmental Science and Technology* 52(9):1449-1490, doi:10.1080/10643389.2020.1859271.

CC BY-NC 4.0 | Attribution-NonCommercial 4.0 International

Kasim, M.R. 2016. *Macroalgae: Study of Biology, Ecology, Utilization and Cultivation.* Jakarta, Swadaya Publishers (*in Indonesian*).

Kilowasid, L.M.H., Manik, D.S., Nevianti, Komang, G.A., Mutmainna, P., Afa, L.O., Rakian, T.C., Hisein, W. S.A., Ramadhan, L.O.A.N. and Alam, S. 2023. The quality of acid soils treated with seaweed (*Kappapychus alvarezii*) sap enriched biochar from Southeast Sulawesi, Indonesia. *Journal of Degraded and Mining Lands Management* 10(2):4255-4265, doi:10.15243/jdmlm.2023.102.4255.

Kinney, T.J., Masiello, C.A., Dugan, B., Hockaday, W.C., Dean, M.R., Zygourakis, K. and Barnes, R.T. 2012. Hydrologic properties of biochars produced at different temperatures. *Biomass and Bioenergy* 41:34-43, doi:10.1016/j.biombioe.2012.01.033.

Kow, K.W., Yusoff, R., Aziz, A.R.A. and Abdullah, E.C. 2014. Characterisation of bio-silica synthesised from cogon grass (Imperata cylindrica). *Powder Technology* 254:206-213, doi:10.1016/j.powtec.2014.01.018.

Kulasinski, K., Guyer, R., Keten, S., Derome, D. and Carmeliet, J. 2015. Impact of moisture adsorption on structure and physical properties of amorphous biopolymers. *Macromolecules* 48(8):2793-2800, doi:10.1021/acs.macromol.5b00248.

Lee, K.Y. and Mooney, D.J. 2012. Alginate: properties and biomedical applications. *Progress in Polymer Science* 37(1):106-126, doi:10.1016/j.progpolymsci.2011.06.003.

Li, H. and Tan, Z. 2021. Preparation of high water-retaining biochar and its mechanism of alleviating drought stress in the soil and plant system. *Biochar* 3(4):579-590, doi:10.1007/s42773-021-00107-0.

Liu, X., Liao, J., Song, H., Yang, Y., Guan, C. and Zhang, Z. 2019. A biochar-based route for environmentally friendly controlled release of nitrogen: urea-loaded biochar and bentonite composite. *Scientific Reports* 9(1):9548, doi:10.1038/s41598-019-46065-3.

Lü, S., Feng, C., Gao, C., Wang, X., Xu, X., Bai, X., Gao, N. and Liu, M. 2016. Multifunctional environmental smart fertilizer based on l -aspartic acid for sustained nutrient release. *Journal of Agricultural and Food Chemistry* 64(24):4965-4974, doi:10.1021/acs.jafc.6b01133.

Ma, Z., Yang, Y., Wu, Y., Xu, J., Peng, H., Liu, X., Zhang, W. and Wang, S. 2019. In-depth comparison of the physicochemical characteristics of biochar derived from biomass pseudo components: Hemicellulose, cellulose, and lignin. *Journal of Analytical and Applied Pyrolysis* 140:195-204, doi:10.1016/j.jaap.2019.03.015.

Madung, Z., Soloi, S., Majid, M.H.A. and Sarjadi, M.S. 2022. Production and characterization of *Imperata cylindrica* paper using potassium hydroxide as a pulping agent. *Biodiversitas* 23(3):1490-1494, doi:10.13057/biodiv/d230337.

Martín-del-Campo, A., Fermín-Jiménez, J.A., Fernández-Escamilla, V.V., Escalante-García, Z.Y., Macías-Rodríguez, M.E. and Estrada-Girón, Y. 2021. Improved extraction of carrageenan from red seaweed (*Chondracantus canaliculatus*) using ultrasound-assisted methods and evaluation of the yield, physicochemical properties and functional groups. *Food Science and Biotechnology* 30(7):901-910, doi:10.1007/s10068-021-00935-7.

Michael, P.S. 2020. Cogon grass biochar amendment and *Panicum coloratum* planting improve selected properties of sandy soil under humid lowland tropical climatic conditions. *Biochar* 2(4):489-502, doi:10.1007/s42773-020-00057-z.

Mujtaba, G., Hayat, R., Hussain, Q. and Ahmed, M. 2021. Physio-chemical characterization of biochar, compost and co-composted biochar derived from green waste. *Sustainability* 13(9):4638, doi:10.3390/su13094628.

Nain, P., Purakayastha, T.J., Sarkar, B., Bhowmik, A., Biswas, S., Kumar, S., Shukla, L., Biswas, D.R., Bandyopadhyay, K.K., Agarwal, B.K. and Saha, N. Das. 2022. Nitrogen-enriched biochar co-compost for the amelioration of degraded tropical soil. *Environmental Technology*, doi:10.1080/09593330.2022.2103742.

Nandiyanto, A.B.D., Oktiani, R. and Ragadhita, R. 2019. How to read and interpret FTIR spectroscope of organic material. *Indonesian Journal of Science and Technology* 4(1):97-118, doi:10.17509/ijost.v4i1.15806.

Nazri, N.A.M., Halim, S.N.Q.S.A. and Karim, S. 2023. Biochar-based graphitic carbon nitride derived from biomass waste for degradation of pyrene. *Advanced Structured Materials* 165, doi:10.1007/978-3-031-21959-7_5.

Niu, Y., Lv, Y., Zhang, X., Wang, D., Li, P. and Hui, S. 2019. Effects of water leaching (simulated rainfall) and additives (KOH, KCl, and SiO_2) on the ash fusion characteristics of corn straw. *Applied Thermal Engineering* 154:485-492, doi:10.1016/j.applthermaleng.2019.03.124.

Panagea, I.S., Berti, A., Čermak, P., Diels, J., Elsen, A., Kusá, H., Piccoli, I., Poesen, J., Stoate, C., Tits, M., Toth, Z. and Wyseure, G. 2021. Soil water retention as affected by management induced changes of soil organic carbon: Analysis of long-term experiments in Europe. *Land* 10(12):1362, doi:10.3390/land10121362.

Phuong, D.T.M. and Loc, N.X. 2022. Rice straw biochar and magnetic rice straw biochar for safranin O adsorption from aqueous solution. *Water* 14(2):186, doi:10.3390/w14020186.

Pramanick, B., Brahmachari, K., Kar, S. and Mahapatra, B.S. 2020. Can foliar application of seaweed sap improve the quality of rice grown under rice–potato–green gram crop sequence with better efficiency of the system? *Journal of Applied Phycology* 32(5):3377-3386, doi:10.1007/s10811-020-02150-z.

Purwanto, S., Gani, R.A. and Suryani, E. 2021. Characteristics of Ultisols derived from basaltic andesite materials and their association with old volcanic landforms in Indonesia. *Sains Tanah* 17(2):135-143, doi:10.20961/STJSSA.V17I2.38301.

Qi, J., Markewitz, D., McGuire, M.A., Samuelson, L. and Ward, E. 2020. Throughfall reduction × fertilization: deep soil water usage in a clay rich Ultisol under Loblolly pine in the Southeast USA. F*rontiers in Forests and Global Change* 2, doi:10.3389/ffgc.2019.00093.

Rajivgandhi, G.N., Kanisha, C.C., Ramachandran, G., Manoharan, N., Mothana, R.A., Siddiqui, N.A., Al-Rehaily, A.J., Ullah, R. and Almarfadi, O.M. 2021. Phytochemical screening and anti-oxidant activity of *Sargassum wightii* enhances the anti-bacterial activity against *Pseudomonas aeruginosa*. *Saudi Journal of Biological Sciences* 28(3):1763-1769, doi:10.1016/j.sjbs.2020.12.018.

Sackey, E.A., Song, Y., Yu, Y. and Zhuang, H. 2021. Biochars derived from bamboo and rice straw for sorption of basic red dyes. *PLoS ONE* 16:0254637, doi:10.1371/journal.pone.0254637.

Sakhiya, A.K., Anand, A. and Kaushal, P. 2020. Production, activation, and applications of biochar in recent times.

CC BY-NC 4.0 | Attribution-NonCommercial 4.0 International

Biochar 2(3):253-285, doi:10.1007/s42773-020-00047-1.

Shitole, S.S., Balange, A.K. and Gangan, S.S. 2014. Use of seaweed (*Sargassum tenerrimum*) extract as gel enhancer for lesser sardine (*Sardinella brachiosoma*) surimi. International *Aquatic Research* 6(1):55, doi:10.1007/s40071-014-0055-9.

Singh, R., Dutta, R.K., Naik, D.V., Ray, A. and Kanaujia, P.K. 2021. High surface area eucalyptus wood biochar for the removal of phenol from petroleum refinery wastewater. *Environmental Challenges* 5:100353, doi:10.1016/j.envc.2021.100353.

Sornhiran, N., Aramrak, S., Prakongkep, N. and Wisawapipat, W. 2022. Silicate minerals control the potential uses of phosphorus-laden mineral-engineered biochar as phosphorus fertilizers. *Biochar* 4(1), doi:10.1007/s42773-021-00129-8.

Sukarman, Saidy, A.R., Rusmayadi, G., Adriani, D.E., Primananda, S., Suwardi, Wirianata, H. and Fitriana, C.D.A. 2022. Effect of water deficit of Ultisols, Entisols, Spodosols, and Histosols on oil palm productivity in Central Kalimantan. *Sains Tanah* 19(2):180-191, doi:10.20961/stjssa.v19i2.65455.

Susanto, A.H. and Dwiati, M. 2022. Short sommunication: Assessment of cogongrass (*Imperata cylindrica* (L.) P.Beauv.) genetic variation in Java, Indonesia using atpB-rbcL and trnL-F intergenic spacer. *Biodiversitas* 23(5):2760-2767, doi:10.13057/biodiv/d230558.

Syahrinudin, Denich, M., Becker, M., Hartati, W. and Vlek, P.L.G. 2020. Biomass and carbon distribution on *Imperata cylindrica* grasslands. *Biodiversitas* 21(1):74-79, doi:10.13057/biodiv/d210111.

Vaghela, P., Trivedi, K., Anand, K.G.V., Brahmbhatt, H., Nayak, J., Khandhediya, K., Prasad, K., Moradiya, K., Kubavat, D., Konwar, L.J., Veeragurunathan, V., Grace, P.G. and Ghosh, A. 2023. Scientific basis for the use of minimally processed homogenates of *Kappaphycus alvarezii* (red) and *Sargassum wightii* (brown) seaweeds as crop biostimulants. *Algal Research* 70:102969, doi:10.1016/j.algal.2023.102969.

Wadduwage, J., Liu, H., Egidi, E., Singh, B.K. and Macdonald, C.A. 2023. Effects of biostimulant application on soil biological and physicochemical properties: A field study. *Journal of Sustainable Agriculture and Environment* 2(3):285-300, doi:10.1002/sae2.12057.

Wang, B., Gao, B. and Fang, J. 2017. Recent advances in engineered biochar productions and applications. Critical *Reviews in Environmental Science and Technology* 47(22), doi:10.1080/10643389.2017.1418580.

Waqas, M., Aburiazaiza, A.S., Miandad, R., Rehan, M., Barakat, M.A. and Nizami, A.S. 2018. Development of biochar as fuel and catalyst in energy recovery technologies. *Journal of Cleaner Production* 188:477-488, doi:10.1016/j.jclepro.2018.04.017.

Weber, P.L., Blaesbjerg, N.H., Moldrup, P., Pesch, C., Hermansen, C., Greve, M.H., Arthur, E. and de Jonge, L.W. 2023. Organic carbon controls water retention and plant available water in cultivated soils from South Greenland. *Soil Science Society of America Journal* 87(2):203-215, doi:10.1002/saj2.20490.

Wystalska, K. and Kwarciak-Kozlowska, A. 2021. The effect of biodegradable waste pyrolysis temperatures on selected biochar properties. *Materials* 14(7):1644, doi:10.3390/ma14071644.

Yaashikaa, P.R., Kumar, P.S., Varjani, S. and Saravanan, A. 2020. A critical review on the biochar production techniques, characterization, stability and applications for circular bioeconomy. *Biotechnology Reports* 28: e00570, doi:10.1016/j.btre.2020.e00570.

Yaich, H., Garna, H., Besbes, S., Barthélemy, J.P., Paquot, M., Blecker, C. and Attia, H. 2014. Impact of extraction procedures on the chemical, rheological and textural properties of ulvan from *Ulva lactuca* of Tunisia coast. *Food Hydrocolloids* 40:53-63, doi:10.1016/j.foodhyd.2014.02.002.

Yang, F., Zhang, G.L., Yang, J.L., Li, D.C., Zhao, Y.G., Liu, F., Yang, R.M. and Yang, F. 2014. Organic matter controls of soil water retention in an alpine grassland and its significance for hydrological processes. *Journal of Hydrology* 519(PD):3086-3093, doi:10.1016/j.jhydrol.2014.10.054.

Yang, Y., Wu, J., Zhao, S., Mao, Y., Zhang, J., Pan, X., He, F. and van der Ploeg, M. 2021. Impact of long-term sub-soiling tillage on soil porosity and soil physical properties in the soil profile. *Land Degradation and Development* 32(10):2892-2905, doi:10.1002/ldr.3874.

Yudina, A. and Kuzyakov, Y. 2023. Dual nature of soil structure: the unity of aggregates and pores. *Geoderma* 434:116478, doi:10.1016/j.geoderma.2023.116478.

Zhang, J., Chi, F., Wei, D., Zhou, B., Cai, S., Li, Y., Kuang, E., Sun, L. and Li, L.J. 2019. Impacts of long-term fertilization on the molecular structure of humic acid and organic carbon content in soil aggregates in black soil. *Scientific Reports* 9(1):11908, doi:10.1038/s41598-019-48406-8.

Zhao, J.J., Shen, X.J., Domene, X., Alcañiz, J.M., Liao, X. and Palet, C. 2019. Comparison of biochars derived from different types of feedstock and their potential for heavy metal removal in multiple-metal solutions. *Scientific Reports* 9(1):9869, doi:10.1038/s41598-019-46234-4.

CC BY-NC 4.0 | Attribution-NonCommercial 4.0 International